Full-Wave Analysis of Shielded Microstrip Lines on Dielectric Substrates using the Characteristic Impedance Computations with Loaded Dielectrics by Finite Element Method

Abdul M. Syed (*)

Dept. of Electrical and Computer Engineering (ECE)
University of Massachusetts Lowell (UML)
Lowell, USA
(*) Corresponding author: sdabdul3@gmail.com

Professor Kanti Prasad

Dept. of Electrical and Computer Engineering (ECE)
University of Massachusetts Lowell (UML)
Lowell, USA
kanti_prasad@uml.edu

Abstract — *Bandpass Filters (BPF) designed using Microstrip Lines (MLIN) and Coupled Microstrip Lines (MCLIN) find applications in the frontend modules of MMIC communication chipsets. Specifically BPF's based on MCLIN design in Band G (4-6 GHz) of Microwave regime and current Long Term Evolution (LTE) Band 46 emphasizes the selection of substrates based on trade-off between MMIC transmission medium loss metrics. In this paper we present a comparative study of return loss, insertion loss of the MLIN's realized with most common dielectric substrates at a operating frequency of 5.15 GHz. Finite Element Method (FEM) based Computational Electromagnetic analysis of shielded MLIN is discussed thoroughly. The characteristic impedance of shielded MLIN achieved using a computer program for FEM based Quasi-Static analysis for ten different substrates are shown. Using Keysight's RF ADS simulator, the Full-Wave results of return and insertion losses for shielded MLIN are presented. Our theoretical Q-factor results for shielded MLIN are in good agreement with the numerical design models available in literature. Full-Wave analysis presented here provides key parametric details in Wireless Communications for the design of Chebyshev type distributed model BPF response using cascaded (parallel) MCLIN's, MLIN's.*

Keywords — *Monolithic Microwave Integrated Circuits (MMIC), Computational Electromagnetic, Shielded Microstrip Line, Characteristic Impedance, Capacitance per unit length, Finite Element Method, Bandpass Filter, Quasi-Static and Full-Wave Analysis*

Introduction

Computational Electromagnetics detailing Quasi-Static characteristic impedance (Z_{0m}) calculations of MLIN's using various techniques such as Finite Difference Time Domain (FDTD), Moment method, FEM can be found extensively in literature. For instance the transmission (S_{21}) and reflection (S_{11}) characteristics of an MLIN placed above ground slot, in which the ground slot is formed due to creation of multiple vias in an confined area on multi-layered Printed Circuit Board (PCB) are given by [1] in 2016. Such an MLIN placed above ground slot, can be easily analyzed by FDTD and Multiconductor Transmission Line (MTL) methods, whose Z_{0m} can be calculated using the Spectral Domain Approach (SDA) [1]. For shielded MLIN with generalized bi-isotropic dielectric substrate and Tellegen's substrate medium, Quasi-Static analysis involving calculation of effective relative permittivity

(ε_{re}) and Z_{0m} is given by FEM formulation using mesh of rectangular elements [2]. Full-Wave analysis of asymmetric MCLIN is performed using Quasi-Symmetric approach involving modal domain integral method and operator formalism in Hilbert space [3]. The major limitation of the approach given in [3] is with higher dielectric constant values, in that the model is dispersion limited at higher frequencies. Based on a computer program for a homogeneous dielectric media, Z_{0m} of shielded MLIN, and capacitance of MCLIN are computed using Quadric-FEM analysis [4]. This process involved quadric interpolation of E-fields and rigorous computation on six nodes of several triangular elements, which is an exhaustive process. Also the modeling of shielded MLIN using FEM along with calculations of capacitance per unit length, Z_{0m} are presented in [5], with the help of an expensive FEM analysis and multiphysics modeling software COMSOL. For low frequency regime, and assuming the symmetric MCLIN to be lossless, the capacitance of transmission line is frequency independent and MCLIN supports Transverse Electromagnetic (TEM) mode [6]. Further Z_{0m} of MCLIN with static conditions, can be computed rigorously with a modified program of single MLIN's Z_{0m} calculation, and by applying Green's function technique with Fourier integral method or by moment method [6]. Even and odd mode Z_{0m} of MCLIN on a PCB using FDTD model which essentially solves 2D Poisson's equation, can be measured with a Time-domain Reflectometer (TDR) [6]. In 1994, [7]-[8] precisely presented Quasi-Static FEM analysis using triangular elements, with arbitrary metallization cross-section in case of shielded MLIN having rectangular, trapezoidal, and semi-trapezoidal conductor strips [7] along with shielded cylindrical MCLIN [8]. Closed-form of MLIN design equations for Computer-aided Design (CAD) program, circuit optimization procedure and a BPF design are summarized in [9]. We present the FEM analysis that is implemented using a modification of open source program code "PGLANT2" [18] in Matlab [21], in order to calculate the Z_{0m} of MLIN based on FEM principles shown in [17], for faster computational speeds and accuracy. The results obtained can be used in ADS [22] for efficient BPF design using MCLIN's, MLIN's.

Finite Element Method Analysis of MLIN

Among the EM computational methods such as FDTD where iterations are used for steady state analysis (Time domain solutions) or the Moment method which

International Journal of Current Trends in Engineering & Technology
www.ijctet.org, ISSN: 2395-3152
Volume: 04, Issue: 02 (March- April, 2018)

is based on weighted residuals (Sub domain method, Galerkin's method, Method of Least Squares), FEM has gained most popularity and has become an ultimate choice in Applied Electromagnetics designs [14]-[18]. In FEM the algebraic equations given by variation principles in [15] are generated based on the continuous domain which is being divided (discretized) into a mesh of finite elements (with nodes being the vertices of triangular elements).
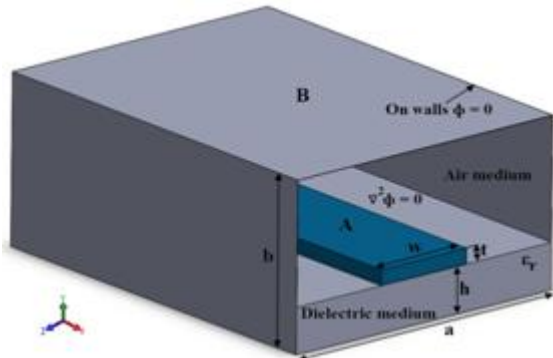

Fig. 1. Microstrip Line in a shielded enclosure [17]

For a shielded MLIN as shown in Fig. 1, exploiting symmetry condition in geometry, the shielded MLIN's cross-section of Fig. 2 (b) is subdivided into half sections as depicted in Fig. 2 (d). The dimensions of shielded MLIN in Fig. 1 are selected as a = 5 mm, b = 3 mm, conductor strip width or line width w = 1.666 mm (2X0.833 mm), substrate height h = 25 mils, thickness of conductor strip (copper foil) t = 0.15 mm. These specifications meet the design conditions of a wide strip line having $\frac{w}{h} \geq 1$ and satisfies Wheeler's incremental inductance rule (t > 4δ, δ being the skin depth) [19]. Using Fig. 2 (d) a mesh having mixed-interpolation type of triangular elements is created as shown in Fig. 3. The 31 Global nodes, 3 Local nodes, and 44 elements are depicted in Fig. 3 by ⬜, n, and 🔵 respectively.
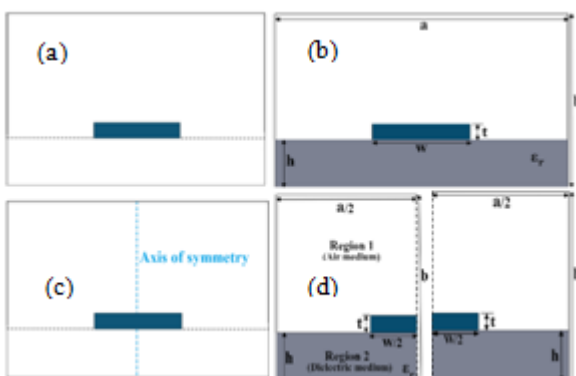

Fig. 2. Shielded Microstrip Line cross-sections in presence of (a). air, (b). loaded dielectric, (c). air media with line of symmetry, and (d). loaded dielectric with symmetrical w/2 strip areas of (b) [17].

Electric Potential φ can be adjusted by minimizing the Electric Field E given by potential of Local nodes inside the triangles with counter clock-wise marking scheme as shown in Fig. 3. Global nodes are assigned to numbers outside of the triangles in Fig. 3, such that the electric energy stored is a functional given by $W_e = \frac{1}{2} CV^2$ [18]. Table (1) shows the Global node coordinates while Table (2) gives Local to Global node connectivity w.r.t each of two regions (Air and Dielectric medium) of Fig. 1, and the 44 elements marked in Fig. 3. The Table (3) (a), and (b) shows information of specified nodes (spn) and free nodes (frn). Using Fig. 3, and Tables (1) to (3) the data array's for computations in Matlab function Program Global Assembly of Node based Triangular Elements version 2 "PGLANT2" [18], are generated. MLIN is classified as an inhomogeneous dielectric medium structure where the dominant mode "Quasi-TEM" mode is supported (TEM mode has $E_z = 0$ and $H_z = 0$). We first consider the mode of propagation as Static or Quasi-TEM mode or Quasi-Static, where the analysis of MLIN assumes a frequency of 0 and the Laplace's equation in cylindrical co-ordinates $\nabla^2 \phi = 0$ is being solved (and this is as such the dominant mode of propagation in transmission line equivalent of Fig. 1). We assume the propagation to occur in Z-direction and the field components have a Z-dependence of the form of $e^{-j\beta z}$. For air medium, permittivity ε = ε_0 and permeability μ = μ_0. The width of MLIN enclosure box or transmission line waveguide 'a' is aligned along x-axis and the cover height 'b' is along y-axis as marked in Fig. 1. Z_{0m} is frequency independent for Quasi-Static case. However to account for the dispersion effects (effect of frequency on Z_{0m} and ε_{re}), we perform Full-Wave analysis using ADS software that solves $\nabla^2 \phi + k^2 \phi = 0$ (Helmholtz equation) using closed-form expressions given in MLIN models of [10]-[13].
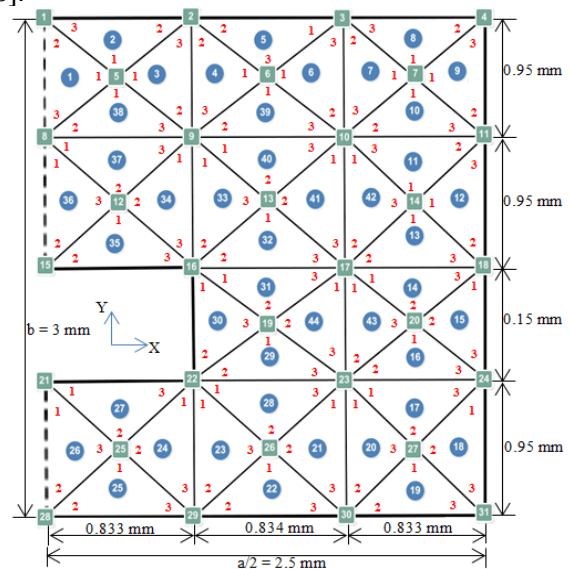

Fig. 3. Mesh of Microstrip structure with symmetrical w/2 strip area in FEM analysis depicting Local nodes, Global nodes, element configurations, and the primary data for Computational Electromagnetics [17]-[18].

Considering Transverse Electric (TE) modes (where H_z exists but $E_z = 0$), the wave function ψ is ψ(x,y) = h_z(x,y) and H_z(x,y,z) = h_z(x,y) $e^{-j\beta z}$. The boundary conditions require that dψ/dx and dψ/dy goes to zero at the boundary walls of x = 0, x = a, y = 0 and y = b i.e, the tangential components of electric and magnetic fields should be continuous for all values of Z in Fig. 1.

International Journal of Current Trends in Engineering & Technology
www.ijctet.org, ISSN: 2395-3152
Volume: 04, Issue: 02 (March- April, 2018)

E and H Field components and ψ can be easily determined using Maxwell's equation and with the aid of built-in models in ADS, that are used to solve partial differential equations and compute these parametric values efficiently. For MLIN, effective relative permittivity ε_{re} is defined in [18]

$$\varepsilon_{re} = \frac{\text{Capacitance of line with substrate material (C)}}{\text{Capacitance of line without substrate material } (C_{air})}$$

where Capacitance is expressed in terms of total energy w_e and voltage V between plates AB of Fig. 1 as $C = \frac{2w_e}{V^2}$. By modifying the Matlab code of "PGLANT" [18] and setting $V_{AB} = 1$ volt, we compile function program twice once with air medium (which gives $C_{air} = 26.626$ pico Farad/m) and then with loaded dielectric media for ten substrates with properties as listed in Table (4), achieving capacitances C values as given in Table (5). Table (5) also shows FEM calculated Quasi-Static Z_{0m} values for each of the substrates of Table (4), using (1) given in [18]

$$Z_{0m} = \frac{1}{c} \cdot \frac{1}{\sqrt{C.C_{air}}} \tag{1}$$

where c is free space velocity of propagation (3×10^8 m/s)

For MLIN of Fig. 1 having a finite strip thickness 't', the effective relative permittivity ε_{re} is given by [10]

$$\varepsilon_{re} = \frac{\varepsilon_r + 1}{2} + \frac{\varepsilon_r - 1}{2} \cdot \frac{1}{\sqrt{1 + 12.(h/w_{eff})}} - \frac{\varepsilon_r - 1}{4.6} \cdot \frac{(t/h)}{\sqrt{w_{eff}/h}} \tag{2}$$

with ε_r being the relative permittivity given in Table (4) for various substrates and the effective strip width w_{eff}

$$w_{eff} = w + \frac{1.25t}{\pi}(1 + \ln\frac{2h}{t}) \tag{3}$$

The values of ε_{re} or $\varepsilon_{re}(0)$ as shown in Table (4), are calculated using (2) and (3) for each of the substrates of Table (4). Table (5) gives the values of $\varepsilon_{re}(f)$, $Z_{0m}(f)$ for an operating frequency f = 5.15 GHz, computed using (4) and (6) respectively. Dispersion relation [12] is given as

$$\varepsilon_{re}(f) = \left[\frac{\sqrt{\varepsilon_r} - \sqrt{\varepsilon_{re}(0)}}{1 + 4F^{-1.5}} + \sqrt{\varepsilon_{re}(0)}\right]^2 \tag{4}$$

where the factor F is

$$F = \frac{4hf\sqrt{\varepsilon_r - 1}}{c}\left\{0.5 + [1 + 2\log(1 + \frac{w}{h})]^2\right\} \tag{5}$$

At HF, the frequency effect on Z_{0m} is given by [13] as

$$Z_0(f) = Z_{0m}(0) \cdot \frac{\varepsilon_{re}(f) - 1}{\varepsilon_{re}(0) - 1}\sqrt{\frac{\varepsilon_{re}(0)}{\varepsilon_{re}(f)}} \tag{6}$$

Fig. 8 and Fig. 9 compares $\varepsilon_{re}(0)$, Z_{om}, $\varepsilon_{re}(f)$, and $Z_{om}(f)$ values using FEM based Quasi-Static Analysis and at f = 5.15 GHz, of the MLIN's designed for various ε_r as given

in Table (5) respectively. For Transverse Magnetic (TM) modes (where E_z exists but $H_z = 0$), the wave function ψ is $\psi(x,y) = e_z(x,y)$ and $E_z(x,y,z) = e_z(x,y) e^{-j\beta z}$. In Fig. 1, if the phase velocity of surface wave and the phase velocity of Quasi-TEM MLIN are in close range of each other, then strong coupling between waves occurs with TM_0, being the lowest order mode. For wider microstrips TE mode exists instead of TM, that will couple strongly with such modes of the MLIN whose lowest coupling frequency is given by [19] as

$$f_s = \frac{c}{(2\pi h)}\sqrt{\frac{2}{(\varepsilon_r - 1)}} * \tan^{-1}\varepsilon_r \tag{7}$$

Transverse resonant mode frequency f_T is given by [19]

$$f_T = \frac{5.9}{(w + 0.4h)\sqrt{\varepsilon_r}} \quad \text{GHz} \tag{8}$$

Quality factor Q of the MLIN, which is a function of substrate thickness 'h' and frequency f (GHz) is the ratio of energy stored to loss, and is one of the MLIN loss metrics and Figure of Merit (FOM) given by (9) [19].

$$\frac{1}{Q} = \frac{1}{Q_c} + \frac{1}{Q_d} + \frac{1}{Q_r} = \frac{1}{Q_0} + \frac{1}{Q_r} = \frac{1}{Q_T} \tag{9}$$

where Q_c, Q_d, Q_r account for the conductor, dielectric, and radiation losses respectively due to discontinuities on MLIN, by surface-wave propagation with frequency given by (7) [19]. In (9), Q_0 is the circuit Q (Loaded Q) while Q or Q_T is total Q (Unloaded Q). Table (6) shows the theoretically calculated f_s and f_T, along with MLIN's Quality factor (Q) values using Closed-loop expressions from the shielded MLIN models given in [19]-[20].

Materials and Methods (Simulations in ADS)

A MLIN circuit schematic view of Fig. 1 is created as shown in Fig. 4 along with an generated layout (Fig. 5), which is then simulated using EM/Momentum ("MomUW") simulations in microwave mode (Full-Wave analysis), with perfect boundary approximations in ADS [22]. For simulation purposes, each of the dielectric substrates from Table (4) is selected with their respective material properties. The parameter entry mode for TLines-Microstrip subcircuit and Simulation-S_Parameters instance in ADS palette is opened and the values as depicted in Fig. 4 for the case of Alumina substrate are entered such that H, Hu (cover height), and T corresponds to h, b, and t respectively as given in Fig. 1. Line length of 5.5 mm (Quarter-wavelength MLIN), line width of w = 1.666mm (FEM based value), and Yamashita et al. dispersion model [12] are assigned to MLIN of Fig. 1.

International Journal of Current Trends in Engineering & Technology
www.ijctet.org, ISSN: 2395-3152
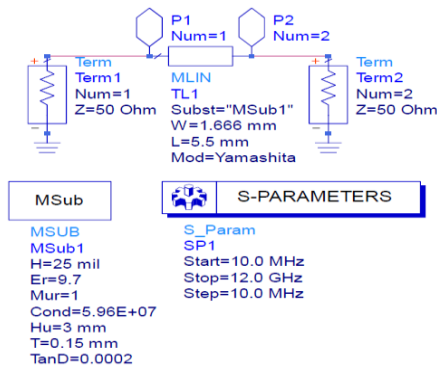**Volume: 04, Issue: 02 (March- April, 2018)**

Fig. 4. Schematic view of MLIN of Fig. 1, with Alumina substrate and input-output port terminations in ADS [22]

Fequency dependent Svensson/Djordjevic dielectric loss model with linear frequency sweep for 1200 points is selected in ADS. A layout as shown in Fig. 5 with appropriate pins for ports is generated by synchronization of entire MLIN design of Fig. 4. Using the ADS EM simulator feature in layout, emModel setup is edited to initialize Momentum ("MomUW") simulations in microwave mode [22]. A FEM symmetry plane is added so as to incorporate Z_{0m} of shielded MLIN with loaded dielectric achieved by FEM.
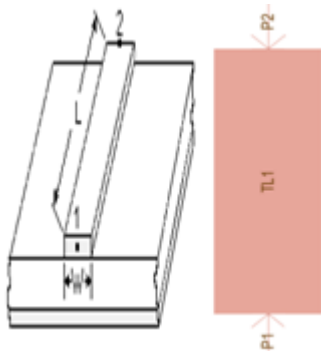

Fig. 5. ADS "LineCalc" utility, Layout generated from schematic view of MLIN (TL1) as shown in Fig. 4 [22]

Global EM simulation option with adaptive frequency plan having 2400 Node points (max), linear extrapolation mode is choosen. Edge mesh having a mesh density of 20 cells per wavelength with "Iterative Dense" [22] matrix sover method, port-solvers are enabled in the simulator. S-Parameter "TML" [22] port calibration with 50 Ω reference impedance for P1 and P2 in Fig. 4 is mapped using the port editor and fulfilling the partitioning rule by descending into layout. Alumina substrate is then created as shown in Fig. 6 by selecting the technology drop-down menu and editing the desired material properties using material definitions submenu. Cover is defined with perfect conductor material, while the interface is a strip plane with mapped layers. Conductor layer is sheet of copper with orientation angle 90° above interface and substrate layer is defined such that bounding area layers are inherited from the designed substrate.
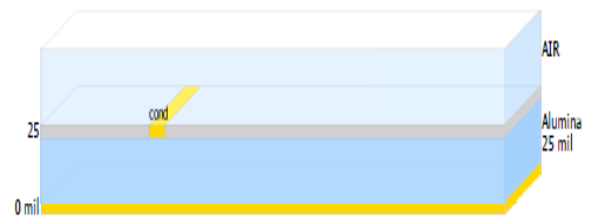

Fig. 6. "MSUB" module of Fig. 4 for Alumina substrate with mapped conductor, cover and layers in ADS [22]

Copper foil of thickness 0.15 mm (4.28 ounces) having electrical conductivity of $5.96X10^7$ S/m is taken as the strip conductor. A small amount of loss tangent (tan δ) is included in obtaining practical simulations to take into account dissipation of each of the MLIN's distributed elements, as per an equivalent microstrip Quarter-wavelength input-output matching transformer. Port coefficient is k = 7.23, for length L and width w of MLIN Quarter-wave matching sections. These act as a planar microstrip resonators having source, load impedances of 50 Ω each for input- output sections, with loaded stripline (Perfect Electric Conductor-PEC, having metallization thickness t = 0.15 mm) needed for excitations.
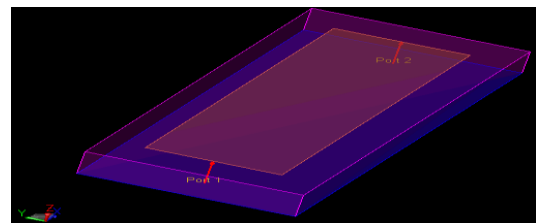

Fig. 7. Momentum "MomUW" 3D Isometric view with conductor, and substrate (Fig. 6) of the MLIN (Fig. 4) using emModel wireframe mode in ADS [22]

MLIN's parametric details combined with defined conductor, substrate and port characteristics in emModel setup is viewed using ADS-3D view as shown in Fig. 7. An optimization scheme for the Line length L is employed along with design verification and design for testability including the verify DRC, netlists matching condition before we started ADS simulations. For effective transmission (S_{21}) and minimal reflection (S_{11}) characteristics, the optimized Line length (l_1) achieved for practical design tolerant thickness is given in Table (7) for case of MLIN's designed with various substrates. To meet MMIC Yield and Reliability requirements of the designed MLIN's for fabrication purposes, we adopted a statistical approach where Log-Normal distribution and Cumulative Distribution Functions (CDF) are used. We used a data-fitting technique for 10 MMIC devices comprising of MLIN, MCLIN's in cascade that provides BPF response. Then using the Matlab's Statistics and Machine Learning tool box (SML) [21], with a model test program we performed accelerated aging at elevated temperatures such that a different device fails at each of the 6 test times namely 400, 800, 1800, 2800, 3800, and 4600 hours. Device Under Test (DUT) is tested for electrical characteristics every 100 hours with SML. After 6000 hours, 4 out of 10 devices were still operating, when

International Journal of Current Trends in Engineering & Technology
www.ijctet.org, ISSN: 2395-3152
Volume: 04, Issue: 02 (March- April, 2018)

the DUT is removed from testing inside SML's created functionality test program. A scale parameter value (σ) or standard deviation of Log-Normal distribution of 1.78 was achieved. Also with a median life of 8×10^5 hours (≈ 91 years), the expected fraction of failed systems in 10 years period, with a CDF or Failure function of 10 FIT (1 FIT = 1 Failure/10^9 Device-hour) was calculated to be 0.2314. A Reliability of 76.86 % is thus projected for our MLIN design based MMIC devices which fits ± 3σ, the Design for Manufacturing (DFM) criterion in microelectronics fabrication.

FEM–Computational Electromagnetics Data

Table (1) Coordinates of Node connections (mm) [17]

Node No. N_n	x coordinate x_n	y coordinate y_n
1	0	3
2	0.833	3
3	1.667	3
4	2.5	3
5	0.417	2.525
6	1.25	2.525
7	2.083	2.525
8	0	2.05
9	0.833	2.05
10	1.667	2.05
11	2.5	2.05
12	0.417	1.575
13	1.25	1.575
14	2.083	1.575
15	0	1.1
16	0.833	1.1
17	1.667	1.1
18	2.5	1.1
19	1.25	1.025
20	2.083	1.025
21	0	0.95
22	0.833	0.95
23	1.667	0.95
24	2.5	0.95
25	0.417	0.475
26	1.25	0.475
27	2.083	0.475
28	0	0
29	0.833	0
30	1.667	0
31	2.5	0

Table (2) Local and Global node system [17]

Element No. N_e	Region No.: 1 = Air, 2 = Dielectric	Local to Global Nodes connectivity		
		n1L (1)	n2L (2)	n3L (3)
1	1	5	1	8
2	1	5	2	1
3	1	5	9	2
4	1	6	2	9
5	1	3	2	6
6	1	6	10	3
7	1	7	3	10
8	1	7	4	3
9	1	7	11	4
10	1	7	10	11
11	1	14	11	10
12	1	14	18	11
13	1	14	17	18
14	1	17	20	18
15	1	18	20	24
16	1	20	23	24
17	2	23	27	24
18	2	24	27	31

Table (2) Local and Global node system [17] (Cont'd.)

Element No. N_e	Region No.: 1 = Air, 2 = Dielectric	Local to Global Nodes connectivity		
		n1L (1)	n2L (2)	n3L (3)
19	2	27	30	31
20	2	23	30	27
21	2	23	26	30
22	2	26	29	30
23	2	22	29	26
24	2	22	25	29
25	2	25	28	29
26	2	21	28	25
27	2	21	25	22
28	2	22	26	23
29	1	19	22	23
30	1	16	22	19
31	1	16	19	17
32	1	13	16	17
33	1	9	16	13
34	1	9	12	16
35	1	12	15	16
36	1	8	15	12
37	1	8	12	9
38	1	5	8	9
39	1	6	9	10
40	1	9	13	10
41	1	10	13	17
42	1	10	17	14
43	1	17	23	20
44	1	17	19	23

Table (3) (a). Specified nodes (spn), and Potentials (V_{spn}) for Dirichlet type Boundary Conditions [17]

Node No. (spn)	Region No.: 1 = Air, 2 = Dielectric	Specified Potential V_{spn} (volts)
1	1	0
2	1	0
3	1	0
4	1	0
8	1	0
11	1	0
15	2	1

International Journal of Current Trends in Engineering & Technology
www.ijctet.org, ISSN: 2395-3152
Volume: 04, Issue: 02 (March- April, 2018)

16	2	1
18	1	0
21	2	1
22	2	1
24	1	0
28	1	0
29	1	0
30	1	0
31	1	0

Table (3) (b). Free nodes (frn), with unspecified Potentials for Neumann type Boundary Conditions

Node No.'s (frn) [N]	5, 6, 7, 9, 10, 12, 13, 14, 17, 19, 20, 23, 25, 26, 27
Free nodes Potentials	Unspecified

Table (4) Dielectric Substrate Properties

ε_r	ε_{re} (0)	ε_{re} (f)	C (pF/m)	Z_{0m} (Ω)	Z_{0m} (f) (Ω)
12.3	8.820	9.256	183.560	47.68	49.13
11.7	8.396	8.796	175.242	48.79	50.24
11.2	8.049	8.418	168.310	49.79	51.23
10.5	7.570	7.898	158.608	51.29	52.72
10.2	7.359	7.670	154.448	51.97	53.39
9.7	7.013	7.297	147.518	53.18	54.59
4.3	3.281	3.336	72.748	75.73	76.91
3.4	2.658	2.690	60.322	83.17	84.26
2.35	1.932	1.944	45.872	95.37	96.31
2.20	1.824	1.834	43.816	97.59	98.50

Table (5) Quasi-Static values using FEM based program

Substrate material	ε_r	(tan δ) Dielectric loss tangent at 10 GHz
(1). GaAs	12.3	0.0016
(2). Si	11.7	0.0050
(3). RO 3010	11.2	0.0022
(4). RT Duroid 6010	10.5	0.0015
(5). 3M EPSILAM 10/ Keene DI-Clad 810	10.2	0.0015
(6). Alumina	9.7	0.0002
(7). FR-4/TMM4	4.3	0.0180
(8). RO 4003C	3.4	0.0020
(9). RT Duroid 5870	2.35	0.0012
(10). RT Duroid 5880	2.20	0.0009

Table (6) Theoretical Microstrip FOM values using Closed-loop expressions of models given in [9]-[13].

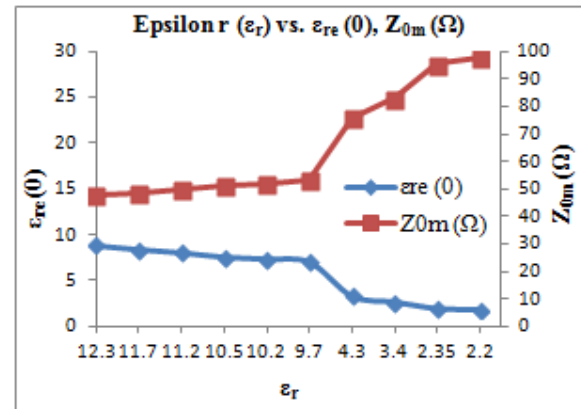| ε_r	Q_0	Q_r	Q_T	f_s (GHz)	f_T (GHz)
12.3	242.71	972.87	194.24	47.120	22.250
11.7	332.15	231.18	136.30	48.291	22.816
11.2	213.42	926.96	173.47	49.330	23.320
10.5	250.07	894.46	195.43	50.910	24.080
10.2	250.43	881.18	195.00	51.640	24.430
9.7	365.83	857.61	256.44	53.000	25.058
4.3	52.946	559.19	48.366	78.570	37.636
3.4	238.44	386.35	147.44	88.180	42.320
2.35	297.01	441.49	177.55	106.93	50.910
2.20	323.77	429.48	184.60	111.06	52.610

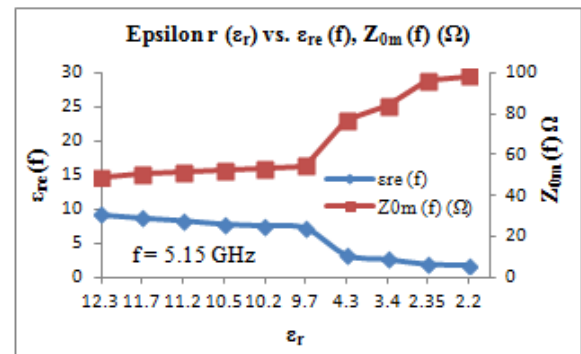Fig. 8. ε_{re} (0), Z_{om} using Quasi-Static Analysis of MLIN

Fig. 9. ε_{re} (f), Z_{om} (f) using MLIN's Quasi-Static Analysis

Results, Loss Characterization of Microstrip

Table (7) gives individual ADS simulation results for an optimized MLIN Line length l_1, while Fig. 10, and Fig. 11 shows the combined ADS results for all substrates of Table (4). Apart from losses Q_c, Q_d, Q_r, the Average Power Handling Capacity (APHC) of MLIN is an important design factor dictated by thermal conductivity of substrate and temperature dependency of strip conductor [20]. From the results given in Table (7), we can infer that a trade-off exists between S_{11}, l_1 and IL values. However in case of Alumina, Line length achieved using "LineCalc" utility of ADS provided an optimized value for S_{11}, and IL as given in Table (7), while conceiving better APHC feature to handle about 5 kW of Continuous Wave (CW) power at 10 GHz [19].

Table (7) Full-Wave results using ADS

Substrate material	Length l_1 (mm)	S_{11} (dB)	IL (dB)

International Journal of Current Trends in Engineering & Technology
www.ijctet.org, ISSN: 2395-3152
Volume: 04, Issue: 02 (March- April, 2018)

(1). GaAs	5.466460	-4.503	-1.931
(2). Si	5.594220	-4.735	-1.834
(3). RO 3010	5.713580	-4.938	-1.711
(4). RT Duroid 6010	5.890040	-5.281	-1.550
(5). 3M EPSILAM 10/ Keene DI-Clad 810	5.970130	-5.449	-1.481
(6). Alumina	6.112780	-5.758	-1.353
(7). FR-4/TMM4	8.713920	-16.06	-0.186
(8). RO 4003C	9.601650	-24.16	-0.027
(9). RT Duroid 5870	11.03720	-24.96	-0.022
(10). RT Duroid 5880	11.301400	-22.63	-0.032

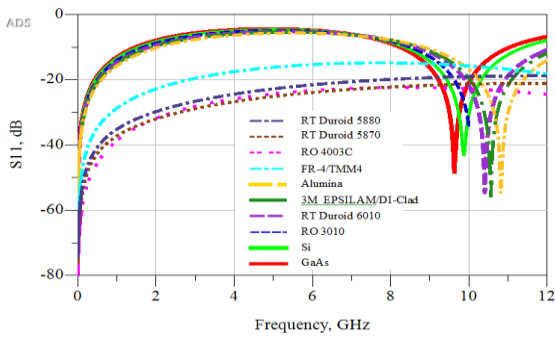| ε_r	Gain (dBi)	Directivity (dBi)	Radiation Efficiency (%)	EIRP (µw)
12.3	-3.84	5.420	11.85	0.430
11.7	-6.92	5.434	5.81	0.207
11.2	-4.54	5.447	10.01	0.353
10.5	-3.59	5.468	12.41	0.431
10.2	-3.56	5.478	12.47	0.429
9.7	-0.94	5.496	22.67	0.771
4.3	-10.5	5.976	2.21	0.066
3.4	-2.55	6.229	13.23	0.386
2.35	-1.73	6.762	14.11	0.403
2.20	-1.49	6.881	14.54	0.413

Fig. 10. Return Loss (S_{11}) using Full-Wave Simulations

Parametric results for the case study of Alumina substrate based MLIN, are given by Fig. 12, Fig. 13, and Fig. 14. Also the Effective Isotropic Radiated Power (EIRP) which is signal output power due to its concentration into a confined area by antenna parameters is given in [19]. EIRP = $[P_T – L_c + G_a]$
                    (10)
where P_T = Output Transmitter power in dBm, L_c = Cable loss in dB and G_a = Antenna Gain in dBi
Neglecting L_c for MLIN case, the antenna parameters including EIRP from the post-processed results of ADS emModel for various substrates are shown in Table (8).
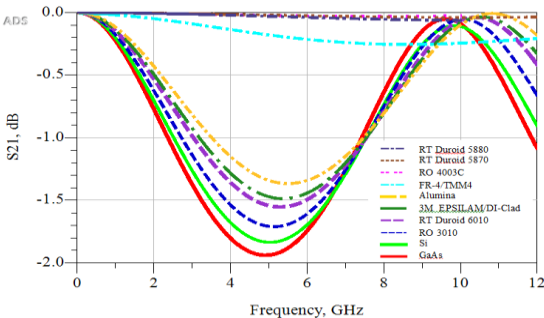

Fig. 11. Insertion Loss (S_{21}) using Full-Wave Simulations

Table (8) Antenna parameters measured using ADS EM-Momentum setup of isotropic (point source) input 4-8 µw
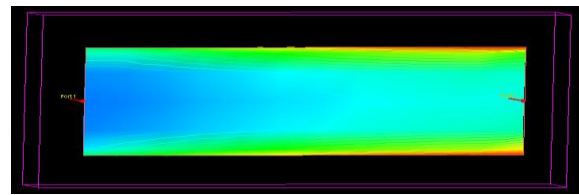

Fig. 12. Port 1 to port 2, post-processed E Field - Momentum visualization of MLIN for Alumina substrate
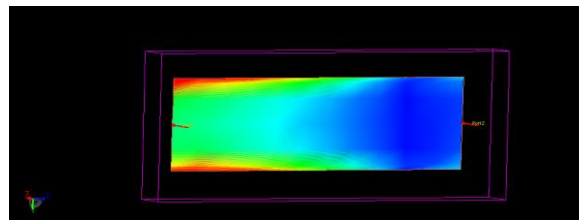

Fig. 13. Port 2 to port 1, post-processed E Field - Momentum visualization of MLIN for Alumina substrate
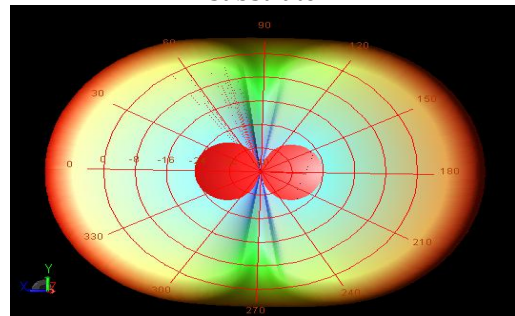

Fig. 14. Far Field computation from the simulation post-results of Alumina substrate using ADS emModel setup

Conclusions

We presented the FEM analysis of shielded MLIN that can be implemented using a Matlab code for higher accuracy and faster computational speeds in Applied Electromagnetic applications, followed by Full-Wave simulations in ADS. EM/Momentum (Full-Wave) results such as Line length (l_1), transmission (S_{21}) and reflection (S_{11}) characteristics in ADS will assist in efficient BPF, MMIC design applications based on MLIN, MCLIN for frontend modules in consumer wireless like smartphones. Increased demands of simultaneous compact shared antennas capabilities to combine multiple carriers' a.k.a "Carrier Aggregation" in

International Journal of Current Trends in Engineering & Technology
www.ijctet.org, ISSN: 2395-3152
Volume: 04, Issue: 02 (March- April, 2018)

Wireless community coupled with custom BPF requirements in the frontend modules at LTE bands can also be addressed by incorporating MLIN features in next Generation wireless communications. Finally using the MLIN realized with Alumina substrate at an operating frequency of 5.15 GHz, we achieved a small improvement in antenna radiation efficiency of $\sim$ 23 % (compared with other dielectrics in our study). We obtained an EIRP value of 0.77 µw by excitation with an isotropic point source using ADS emModel setup for an MLIN based on Alumina substrate whose Far Field pattern, and E-Fields are post-processed.

Acknowledgment

References

[1] K. Takamatsu, T. Tobana, Y. Isota and T. Sasamori, "Analysis of transmission characteristic of a microstrip line placed above a ground slot," *2016 International Symposium on Electromagnetic Compatibility - EMC EUROPE*, Wroclaw, 2016, pp. 94-99.

[2] Z. J. Mancic and V. V. Petrovic, "Quasi-static analysis of the shielded microstrip line with bi-isotropic substrate by the strong FEM formulation," *2013 11th International Conference on Telecommunications in Modern Satellite, Cable and Broadcasting Services (TELSIKS)*, Nis, 2013, pp. 513-516.

[3] A. Khodja, R. Touhami, M. C. E. Yagoub and H. Baudrand, "Full-wave modal analysis of asymmetric coupled lines using the quasi-symmetric approach," *2011 11th Mediterranean Microwave Symposium (MMS)*, Hammamet, 2011, pp. 142-145.

[4] C. J. Shuai, "The Quadric FEM analysis of characteristic impedance in microstrip line of homogeneous dielectric," *Proceedings of 2011 Cross Strait Quad-Regional Radio Science and Wireless Technology Conference*, Harbin, 2011, pp. 79-81.

[5] S. M. Musa and M. N. O. Sadiku, "Modeling of shielded, suspended and inverted, microstrip lines," *IEEE SoutheastCon 2008*, Huntsville, AL, 2008, pp. 309-313.

[6] P. S. Bhattacharjee, S. Das and S. K. Chowdhury, "Characteristics impedance of coupled microstrip lines," *Proceedings of International Symposium on Electromagnetic Compatibility*, Atlanta, GA, 1995, pp. 137-138.

[7] M. S. Alam, K. Hirayama, Y. Hayashi and M. Koshiba, "Analysis of shielded microstrip lines with arbitrary metallization cross section using a vector finite element method," in *IEEE Transactions on Microwave Theory and Techniques*, vol. 42, no. 11, pp. 2112-2117, Nov 1994.

[8] M. A. Kolbehdari, "Quasi-static characteristic of a shielded cylindrical coupled microstrip transmission line by finite-element method," *Southeastcon '94. Creative Technology Transfer - A Global Affair., Proceedings of the 1994 IEEE*, Miami, FL, 1994, pp. 170-174.

[9] S. S. Bedair and M. I. Sobhy, "Accurate formulas for computer-aided design of shielded microstrip circuits," in *Microwaves, Optics and Antennas, IEE Proceedings H*, vol. 127, no. 6, pp. 305-308, December 1980.

[10] I. J. Bahl and R. Garg, "Simple and accurate formulas for a microstrip with finite strip thickness," in *Proceedings of the IEEE*, vol. 65, no. 11, pp. 1611-1612, Nov. 1977.

[11] Erik O. Hammerstad, "Equations for Microstrip Circuit Design," *1975 5th European Microwave Conference*, Hamburg, Germany, 1975, pp. 268-272.

[12] E. Yamashita, K. Atsuki and T. Ueda, "An Approximate Dispersion Formula of Microstrip Lines for Computer-Aided Design of Microwave Integrated Circuits," in *IEEE Transactions on Microwave Theory and Techniques*, vol. 27, no. 12, pp. 1036-1038, Dec 1979.

[13] E. Hammerstad and O. Jensen, "Accurate Models for Microstrip Computer-Aided Design," *1980 IEEE MTT-S International Microwave symposium Digest*, Washington, DC, USA, 1980, pp. 407-409.

[14] Roger F. Harrington, "Time-Harmonic Electromagnetic Fields," Wiley-IEEE Press, New York, 2001.

[15] Jean Van Bladel, "Electromagnetic Fields," 2nd ed, IEEE Press, Wiley-Interscience, New York 2007.

[16] Jian-Ming Jin "Finite Element Method in Electromagnetics," Wiley-IEEE, New York, 2002.

[17] Giuseppe Pelosi, Roberto Coccioli, and Stefano Selleri, "Quick Finite Elements for Electromagnetic Waves," 2nd ed. Artech House, Norwood-MA, 2009.

[18] Dikshitulu K. Kalluri, "Electromagnetic Waves, Materials, and Computation with MATLAB," CRC Press, Taylor and Francis Group, FL, August 2011.

[19] K. C. Gupta, Ramesh Garg, Inder Bahl, and Prakash Bhartia, "Microstrip Lines and Slotlines," 2nd ed. Artech House, Norwood-MA, 1996.

[20] E. Belohoubek and E. Denlinger, "Loss Considerations for Microstrip Resonators," in *IEEE Transactions on Microwave Theory and Techniques*, vol. 23, no. 6, pp. 522-526, Jun 1975.

[21] The Mathworks, "Matlab," UMass. student edition, licensed version 7.10.0.499 64-bit (R2010a), Toolboxes/RF Tools, Natick, MA, 1984-2010.

[22] Keysight's Premier High-Frequency and High Speed Design Platform, "RF and Microwave Design Suite," Advanced Design System (ADS) version 2016.01, Keysight Inc, Englewood, CO, 1985-2016.

Author's Profile

(1) Abdul M. Syed – Received the B. E degree in Electronics and Communication Engineering from Osmania University, India, and M. S degree in Electrical Engineering (EE) with Optoelectronics concentration from UML, USA. Currently he is pursuing Ph. D degree in EE under Prof. Kanti Prasad's advising at UML, USA. He is a Life member of The Institution of Electronics and Telecommunication Engineers (IETE), New Delhi, India.

(2) Professor Kanti Prasad – Dr. Kanti Prasad is a professor in the Department of Electrical and Computer Engineering and is founding Director of Microelectronics/VLSI Technology Laboratories at the University of Massachusetts Lowell (UML). Professor Prasad received his B.Sc. (Agra University), the B.E. (University of Roorkee, IIT now) and Ph.D. (University of South Carolina, USA) degrees. Professor Prasad initiated the Microelectronics/ VLSI program in 1984, and is teaching EECE.5020/4690 VLSI Design, EECE.5040/4070 VLSI Fabrication, and EECE.5170 MMIC Design and Fabrication courses since their inception at UML. Professor Prasad has achieved a rare distinction accorded to any U.S. and Canadian faculty by ASEE inducting him in the Academy of Fellows on 26th June 2013 at its national conference held in Atlanta. Professor Prasad is a Professional Engineer registered in the Commonwealth of Massachusetts, USA. He is the author/co-author of over 150 theses, dissertations and papers published and presented in journals /conferences of national and international repute.